

Contribution from the Department of Chemistry and Molecular Structure Center, Indiana University, Bloomington, Indiana 47405

Halide Abstraction from TiCl_3 by ZnCl_2

KIRSTEN FOLTING, JOHN C. HUFFMAN, RICK L. BANSEMER, and KENNETH G. CAULTON*

Received December 28, 1983

Reaction of TiCl_3 with ZnCl_2 in THF yields a material whose infrared spectrum indicates inequivalent THF units. X-ray diffraction shows this material to be $[\text{trans-Ti}^{\text{III}}\text{Cl}_2(\text{THF})_4][\text{Zn}^{\text{II}}\text{Cl}_3(\text{THF})]$, containing the quasi-tetrahedral anion $\text{ZnCl}_3(\text{THF})^-$. The crystal form is orthorhombic, $P2_12_12_1$, with (-158°C) $a = 21.970(12)\text{ \AA}$, $b = 9.065(3)\text{ \AA}$, $c = 14.134(5)\text{ \AA}$, and $Z = 4$. Conformational features and Ti-O bond lengths are consistent with THF being capable of donating to octahedral Ti(III) with both lone pairs. Structural features of halide compounds containing both an early transition metal and an electropositive metal are reviewed.

Introduction

It is an established fact that inclusion of electropositive metal ions such as Al^{3+} , Mg^{2+} , and Zn^{2+} in recipes for Ziegler-Natta olefin polymerization catalysts substantially alters catalyst performance.¹ For example, one commercial source of titanium for polymerization catalysis is a composition of empirical formula $\text{TiCl}_3 \cdot 1/3\text{AlCl}_3$,² formed by aluminum reduction of TiCl_4 . While a persuasive explanation of the molecular origin of the function of such main-group "cocatalysts" is currently lacking, we hope that structural information on the interaction of electropositive metals with early-transition-metal halides might offer an initial basis for further understanding.

We have recently shown that not simply $\text{VCl}_2(\text{THF})_2$ but instead $[\text{V}_2(\mu\text{-Cl})_3(\text{THF})_6]_2[\text{Zn}_2(\mu\text{-Cl})_2\text{Cl}_4]$ is the surprising product of the zinc metal reduction of $\text{VCl}_3(\text{THF})_3$ in tetrahydrofuran.³ With this finding that zinc(II) chlorides in THF are not merely innocent "spectator" species in the presence of vanadium(II) chlorides, we have begun to investigate directly the reactivity of ZnCl_2 toward early-transition-metal halides. We wish to report here the nature of the nonredox reaction of TiCl_3 with ZnCl_2 in THF.

Experimental Section

General Information. All manipulations were done under a nitrogen atmosphere by using Schlenk techniques or a glovebox. THF was dried with sodium/potassium benzophenone ketyl and distilled prior to use. Anhydrous ZnCl_2 was obtained by the method of Pray⁴ and used throughout. Anhydrous TiCl_3 was commercial "hydrogen-reduced" material (Stauffer).

$\text{TiCl}_3 \cdot \text{ZnCl}_2 \cdot 5\text{THF}$. (a) ZnCl_2 (2.7 g, 20 mmol) and TiCl_3 (6.2 g, 40 mmol) were refluxed in 100 mL of THF for 24 h. The resulting blue-green solution was filtered hot and then allowed to cool to room temperature. After cooling, a pale blue, microcrystalline solid precipitated. This solid was filtered and vacuum dried, yielding 6.0 g (46% based on Zn) of $\text{TiCl}_3 \cdot \text{ZnCl}_2 \cdot 5\text{THF}$. IR (Nujol mull): $\nu(\text{COC})$ 825 (s), 875 (m), 995 (s), 1032 (m) cm^{-1} . (b) Repetition of this reaction using 19 mmol each of ZnCl_2 and TiCl_3 in 100 mL of THF yielded 6.54 g (53%) of a blue solid whose infrared spectrum is identical with that of $\text{TiCl}_3 \cdot \text{ZnCl}_2 \cdot 5\text{THF}$ produced in method a above. The yield here can be increased by concentration of the filtrate.

Crystallization of $\text{TiCl}_3 \cdot \text{ZnCl}_2 \cdot 5\text{THF}$. A 1.0-g sample of $\text{TiCl}_3 \cdot \text{ZnCl}_2 \cdot 5\text{THF}$ from method a above was dissolved in 9 mL of hot THF, yielding a blue-green solution. This solution was slowly cooled by simply turning off the power to the heat source (oil bath). After 1 day starlike clusters of crystals formed. The supernatant solution was

Table I. Crystal Data for $\text{TiCl}_3 \cdot \text{ZnCl}_2 \cdot 5\text{THF}$

formula	$[\text{TiCl}_2(\text{OC}_4\text{H}_8)_4][\text{ZnCl}_3(\text{OC}_4\text{H}_8)]$
color	blue-green
cryst dims, mm	$0.15 \times 0.15 \times 0.13$
space group	$P2_12_12_1$
cell dims (at -158°C ; 30 reflcns)	
<i>a</i> , Å	21.970 (12)
<i>b</i> , Å	9.065 (3)
<i>c</i> , Å	14.134 (5)
molecules/cell	4
vol, Å ³	2814.79
calcd density, g/cm ³	1.536
wavelength, Å	0.710 69
mol wt	651.08
linear abs coeff, cm ⁻¹	16.6
no. of unique intensities	2102
no. of reflcns with $F > 0.0$	2085
no. of reflcns with $F >$ $3.00\sigma(F)$	2040
$R(F)$	0.0527
$R_w(F)$	0.0604
goodness of fit for the last cycle	1.59
max Δ/σ for last cycle	0.05

syringed off and the crystals were dried under vacuum. These crystals have an infrared spectrum identical with that of the microcrystals in part a, above.

Crystallographic Study. A suitable crystal was cleaved from a larger sample and transferred to the goniostat by using standard inert-atmosphere handling techniques. A systematic search of a limited hemisphere of reciprocal space located a set of diffraction maxima of orthorhombic symmetry with axial extinctions corresponding to space group $P2_12_12_1$. Diffraction data were collected (at -158°C ; $6^\circ \leq 2\theta \leq 45^\circ$) and processed according to our usual procedures.⁵ Characteristics of the data collected appear in Table I.

The structure was solved by direct methods and Fourier techniques and refined by full-matrix least squares. An initial data set taken at a scan rate of $8^\circ/\text{min}$ resulted in four of the THF carbon atoms refining to non-positive-definite thermal parameters. A second data set, reported herein, was then collected with a scan rate of $4^\circ/\text{min}$ with 10-s backgrounds. While the results were improved, two of the carbon atoms (C14 and C25) still refined to non-positive-definite thermal parameters. Since the problematic carbons are not those attached to oxygen and since these are the ring positions most susceptible to ring-pucker disorder, we attribute this difficulty to disorder. In addition, several of the hydrogen atoms located in a difference synthesis did not converge. For these reasons, the final cycles included isotropic thermal parameters for C14 and C25 and hydrogen atoms were placed in fixed, idealized positions. No absorption correction was deemed necessary: a ψ scan of several reflections was essentially flat. A final difference Fourier map was featureless, the largest peak being less than $0.4\text{ e}/\text{\AA}^3$. The proper enantiomer for the crystal selected was established by comparison of the R factor for each of the two possibilities.

- (1) (a) Gavens, P. D.; Bottrill, N.; Kelland, J. W.; McMeeking, J. In "Comprehensive Organometallic Chemistry"; Wilkinson, G., Stone, F. G. A., Abel, E. W., Eds.; Pergamon Press: Oxford, 1982; Vol. 3, p 475. (b) See ref 1a, p 522 (Table 8), for patent numbers.
- (2) Reference 1, p 511 ff.
- (3) Bouma, R. J.; Teuben, J. H.; Beukema, W. R.; Bansemer, R. L.; Huffman, J. C.; Caulton, K. G. *Inorg. Chem.* **1984**, *23*, 2715. See also: Cotton, F. A.; Duraj, S. A.; Extine, M. W.; Lewis, G. E.; Roth, W. J.; Schmulbach, C. D.; Schwotzer, W. *J. Chem. Soc., Chem. Commun.* **1983**, 1377.
- (4) Pray, A. R. *Inorg. Synth.* **1957**, *5*, 153.

- (5) Huffman, J. C.; Lewis, L. N.; Caulton, K. G. *Inorg. Chem.* **1980**, *19*, 2755.

Table II. Fractional Coordinates and Isotropic Thermal Parameters for $\text{TiCl}_3 \cdot \text{ZnCl}_2 \cdot 5\text{THF}$

atom	10^4x	10^4y	10^4z	$10B_{\text{iso}}^a$ \AA^2
Zn1	214 (1)	11987 (1)	492 (1)	16
Cl2	1155 (1)	12552 (3)	4429 (2)	20
Cl3	-544 (1)	12591 (4)	3936 (2)	32
Cl4	155 (1)	9738 (3)	5575 (2)	28
O5	72 (3)	13454 (9)	6070 (6)	24
C6	567 (6)	14211 (16)	6572 (10)	33
C7	357 (6)	15732 (14)	6639 (10)	29
C8	-237 (6)	15868 (14)	6139 (10)	29
C9	-470 (5)	14301 (13)	6163 (10)	26
Ti10	2667 (1)	7448 (2)	5443 (1)	11
Cl11	2209 (1)	5882 (3)	6571 (2)	21
Cl12	3141 (1)	9032 (3)	4343 (2)	15
O13	1886 (3)	7528 (9)	4627 (5)	16
C14	1572 (6)	6281 (15)	4261 (9)	27 (3)
C15	1000 (6)	6864 (16)	3815 (10)	31
C16	1170 (6)	8397 (17)	3484 (10)	34
C17	1609 (5)	8920 (14)	4236 (9)	22
O18	3465 (3)	7322 (10)	6210 (5)	23
C19	3773 (6)	6033 (21)	6560 (13)	50
C20	4364 (10)	6455 (30)	6916 (13)	70
C21	4428 (7)	7978 (37)	6833 (14)	87
C22	3797 (7)	8641 (9)	6587 (11)	40
O23	2972 (3)	5609 (9)	4688 (5)	15
C24	3464 (5)	5598 (15)	3955 (9)	25
C25	3594 (6)	3992 (14)	3761 (9)	23 (2)
C26	3003 (6)	3223 (15)	4040 (10)	29
C27	2797 (6)	4050 (12)	4853 (10)	28
O28	2325 (3)	9292 (8)	6166 (5)	13
C29	2511 (6)	10835 (14)	6040 (10)	28
C30	2187 (6)	11646 (15)	6817 (8)	25
C31	1589 (5)	10843 (12)	6862 (8)	15
C32	1763 (5)	9252 (13)	6775 (8)	19

^a Isotropic values for those atoms refined anisotropically are calculated by using the formula given by: Hamilton, W. C. *Acta Crystallogr.* 1959, 12, 609.

Table III. Selected Bond Distances (Å) and Angles (deg) for $[\text{trans-TiCl}_2(\text{THF})_4]^+ [\text{ZnCl}_3(\text{THF})]^-$

Zn-Cl2	2.240 (3)	Ti-Cl12	2.359 (3)
Zn-Cl3	2.239 (3)	Ti-O13	2.069 (7)
Zn-Cl4	2.242 (3)	Ti-O18	2.064 (8)
Zn-O5	2.121 (8)	Ti-O23	2.089 (7)
Ti-Cl11	2.361 (3)	Ti-O28	2.098 (7)
Cl2-Zn-Cl3	115.94 (13)	Cl12-Ti-O13	88.69 (22)
Cl2-Zn-Cl4	112.92 (12)	Cl12-Ti-O18	90.30 (24)
Cl2-Zn-O5	103.29 (23)	Cl12-Ti-O23	90.43 (22)
Cl3-Zn-Cl4	115.83 (14)	Cl12-Ti-O28	89.64 (22)
Cl3-Zn-O5	102.28 (24)	O13-Ti-O18	177.6 (3)
Cl4-Zn-O5	104.26 (27)	O13-Ti-O23	90.6 (3)
Cl11-Ti-Cl12	178.67 (14)	O13-Ti-O28	86.9 (3)
Cl11-Ti-O13	92.51 (22)	O18-Ti-O23	87.2 (3)
Cl11-Ti-O18	88.52 (24)	O18-Ti-O28	95.3 (3)
Cl11-Ti-O23	90.12 (22)	O23-Ti-O28	177.5 (3)
Cl11-Ti-O28	89.87 (23)		

Table IV. Structural Features of THF^- Coordination

	dist of M from COC plane, Å		dist of M from COC plane, Å	
	M-O, Å		M-O, Å	
Ti-O13	2.069 (7)	0.20	Ti-O28	2.098 (7) 0.30
Ti-O18	2.064 (8)	0.16	Zn-O5	2.121 (8) 0.76
Ti-O23	2.089 (7)	0.19		

The results of the structure determination appear in Tables II-IV and Figures 1 and 2. Additional data have been deposited as supplementary material.

Results

The reaction of TiCl_3 with equimolar ZnCl_2 in refluxing THF occurs with deposition of a microcrystalline pale blue

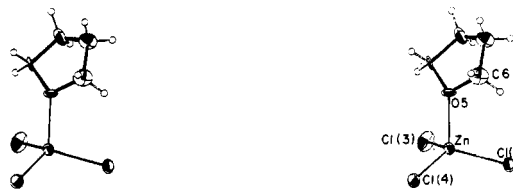
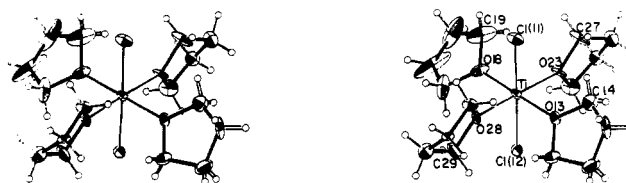


Figure 1. Stereo ORTEP drawings: above, $\text{trans-TiCl}_2(\text{THF})_4^+$; below, $\text{ZnCl}_3(\text{THF})^-$. Unlabeled carbon atoms follow sequentially from the atom labels shown.

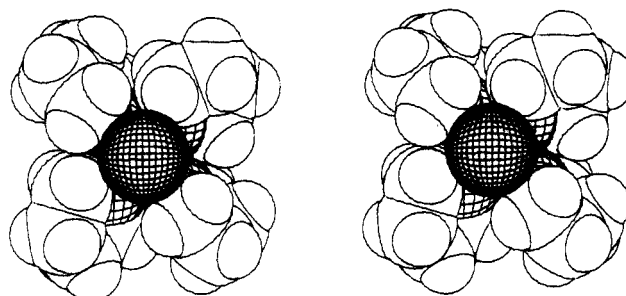


Figure 2. Stereo space-filling drawing of $\text{trans-TiCl}_2(\text{THF})_4^+$: dense hatching, chlorine; open hatching, oxygen. O13 and O18 are in the northeast and southwest quadrants.

solid (1). Since anhydrous TiCl_3 and ZnCl_2 independently react with hot THF to give $\text{mer-TiCl}_3(\text{THF})_3$ and $\text{ZnCl}_2(\text{THF})_2$, respectively, the latter two are probably the actual reactants. The product is somewhat soluble (0.06 M) in THF at 25 °C and more soluble in refluxing THF, from which single crystals may be grown. Solubility in CH_2Cl_2 (in which 1 is stable) is considerably better. Unlike $\text{ZnCl}_2(\text{THF})_2$,⁶ whose crystals lose THF on evacuation at 25 °C, crystals of 1 remain transparent under vacuum at 25 °C and thus appear to be stable to loss of ether.

It appears that the infrared C-O-C stretching modes can be useful in structural assignments of THF complexes. Compound 1 displays a total of four medium-to-strong bands in the O-C singlebond stretching region of the infrared spectrum. We take this to indicate that 1 contains THF molecules in two distinct environments. In contrast, $[\text{V}_2\text{Cl}_3(\text{THF})_6]_2\text{Zn}_2\text{Cl}_6$,³ with but one type of THF, shows only two infrared bands, while $\text{mer-TiCl}_3(\text{THF})_3$ shows three absorptions (1040, 1010, and 845 cm^{-1}), the lowest of which is unusually broad.

The crystal structure of 1 (Figures 1 and 2) shows it to have composition $\text{TiCl}_3 \cdot \text{ZnCl}_2 \cdot 5\text{THF}$ but to be comprised of non-interacting $\text{trans-TiCl}_2(\text{THF})_4^+$ cations and $\text{ZnCl}_3(\text{THF})^-$ anions. The cation is close to octahedral, with Ti and the four ether oxygens coplanar to within 0.01 Å and all Cl-Ti-O angles within 2.5° of 90°. The Ti-Cl distances are equivalent. The quasitetrahedral $\text{ZnCl}_3(\text{THF})^-$ unit shows three equivalent Zn-Cl distances (2.24 Å) and a shorter distance to the ether oxygen (2.12 Å). Nevertheless, the O-Zn-Cl angles (average

103.3°) are smaller than the Cl–Zn–Cl angles (average 114.9°).

Of the four independent THF rings bound to Ti, two are in the envelope conformation (four atoms coplanar) and two are in the half-chair ("twist") conformation. The ring bound to zinc is in a distinct conformation, with the two remote carbons displaced 0.51 and 0.86 Å to the same side of the COC plane. All five oxygen atoms in the structure are pyramidal (see Table IV), but the pyramidality is much greater for O5 (bound to zinc) than for any of those bound to titanium. There is also a correlation of shorter Ti–O distances when the ether oxygen is closer to planarity.

The THF ring planes do not lie in the TiO_4 plane; space-filling models (Figure 2) reveal this to be impossible due to cis repulsions between THF rings. If we define the orientation of the THF rings on titanium by oxygen and the two attached carbons, these planes are rotated 39 and 37° for O13 and O18 and 78 and 72° for O23 and O28. Trans pairs of THF rings rotate such that they remain essentially coplanar (O13/O18 plane dihedral angle is 4°, while that of O23 and O28 is 9°). Consequently, these rings are *not* in phase as they would be in a four-bladed propeller. Note also that the two longer Ti–O bonds correspond to the THF rings rotated more out of the TiO_4 plane; space-filling drawings (Figure 2) indicate that these rings experience greater repulsion from the axial chlorines. These more rotated THF rings may be shown by symmetry arguments to be less capable of π -donation from oxygen lone pairs.

Discussion

Reactivity Patterns. Zinc dichloride in THF acts toward *mer*- $\text{TiCl}_3(\text{THF})_3$ as a chloride-abstracting reagent analogous to Ag^+ or Ti^+ . Rather than formation of a halide-bridged molecular adduct such as $(\text{THF})_3\text{ClTi}(\mu\text{-Cl})_2\text{ZnCl}_2$, halide transfer takes place, and the resultant open coordination site is occupied by THF. This leads to formation of the previously unknown monomeric $\text{ZnCl}_3(\text{THF})^-$ ion rather than the dimeric $\text{Cl}_2\text{Zn}(\mu\text{-Cl})_2\text{ZnCl}_2^{2-}$ ion, which crystallizes from THF with the $\text{V}_2\text{Cl}_3(\text{THF})_6^+$ counterion.³

Both the redox preparation of $[\text{V}_2\text{Cl}_3(\text{THF})_6]_2[\text{Zn}_2\text{Cl}_6]$ and the nonredox preparation of $[\text{TiCl}_2(\text{THF})_4][\text{ZnCl}_3(\text{THF})]$ thus lead to products that lack any direct linkage between zinc and the early transition metal. More common than halide ion abstraction is the formation of molecular adducts with electropositive metal halides. This has been seen in synthetic and structural studies related to the Montedison, Phillips,^{1b} and Mitsui olefin polymerization catalysts. For example, TiCl_4 and MgCl_2 in ethyl acetate yield $\text{TiCl}_4\cdot\text{MgCl}_2\cdot 4\text{EtOAc}$, with both metals octahedral in a structure $\text{Cl}_4\text{Ti}(\mu\text{-Cl})_2\text{Mg}[\text{CH}_3\text{C}(\text{O})\text{OEt}]_4$.⁷ A related material, $\text{TiCl}_3(\text{O}_2\text{CCH}_2\text{Cl})\cdot\text{MgCl}_2\cdot 3\text{ClH}_2\text{CCO}_2\text{Et}$, again has both metals octahedral with connectivity $\text{Cl}_3\text{Ti}(\mu\text{-O}_2\text{CCH}_2\text{Cl})(\mu\text{-Cl})_2\text{Mg}[\text{ClH}_2\text{CC}(\text{O})\text{OEt}]_3$.⁸ The molecular adduct of Ti(III) and tetrahedral aluminum, $\text{Cp}_2\text{Ti}(\mu\text{-Cl})_2\text{AlEt}_2$, was structurally characterized long ago (from heptane solvent).⁹ In benzene, TiCl_4 , hexamethylbenzene, AlCl_3 , and Al^0 react to give $(\eta\text{-C}_6\text{Me}_6)\text{Ti}(\eta^2\text{-AlCl}_4)_2$.¹⁰ Among complexes of the later transition metals $\text{Cl}_2\text{Fe}(\mu\text{-Cl})_2\text{Mg}(\text{THF})_4$ has been crystallized from THF, with Fe(II) tetrahedral and magnesium octahedral.¹¹ The structure of $(\text{Cp}_2\text{TiCl})_2\text{MnCl}_2\cdot 2\text{THF}$, from $(\text{Cp}_2\text{TiCl})_2$ and MnCl_2 in THF, contains pseudotetrahedral Ti(III) and trans-octahedral Mn(II): $\text{Cp}_2\text{Ti}(\mu\text{-Cl})_2\text{Mn}(\text{THF})_2(\mu\text{-Cl})_2\text{TiCp}_2$.¹²

It is probable that at least some of the distinction between the saltlike and molecular products described above is dependent upon whether or not a coordinating ligand is available (e.g. as solvent). Thus, molecular $\text{Cp}_2\text{Ti}(\mu\text{-Cl})_2\text{Zn}(\mu\text{-Cl})_2\text{TiCp}_2$ is formed either by zinc reduction of Cp_2TiCl_2 or from $(\text{Cl}_2\text{TiCl})_2$ and ZnCl_2 , but in benzene. If this compound is dissolved in benzene/1,2-dimethoxyethane, ionic $[\text{Cp}_2\text{Ti}(\text{DME})]_2[\text{Zn}_2\text{Cl}_6]\cdot\text{C}_6\text{H}_6$ may be crystallized.¹³ We have observed that $[\text{TiCl}_2(\text{THF})_4][\text{ZnCl}_3(\text{THF})]$ can be recovered from concentrated solution in CH_2Cl_2 by judicious addition of small amounts of THF. However, addition of pentane brings out only a mixture of colorless and pale blue solids, suggesting loss of coordinated THF and/or segregation of metals into distinct zinc and titanium compounds.

Those examples of halide transfer described above indicate transfer from the early transition metal to the electropositive metal. This behavior is reversed in the 2:1 reaction of $\text{MgCl}_2(\text{THF})_2$ with $\text{TiCl}_4(\text{THF})_2$ in THF solvent.¹⁴ Here $\text{TiCl}_3(\text{THF})^-$ forms, and halide-deficient MgCl^+ condenses with MgCl_2 to give $\text{Mg}_2(\mu\text{-Cl})_3(\text{THF})_6^+$.

This brief review of known bimetallic adducts and salts reveals a distinction between Mg^{2+} , which shows a strong preference for coordination number 6, and Zn^{2+} (smaller than Mg^{2+}) and Al^{3+} , which adopt coordination number 4.

The question of why *trans*- $\text{TiCl}_2(\text{THF})_4^+$ precipitates with the $\text{ZnCl}_3(\text{THF})^-$ ion while $\text{V}_2\text{Cl}_3(\text{THF})_6^+$ precipitates with $\text{Zn}_2\text{Cl}_6^{2-}$ remains open. One rationale derives from the idea that we are seeing only the least soluble product possible and that such a salt has the optimum match of cation with anion size. Thus, the labile equilibrium between $\text{ZnCl}_3(\text{THF})^-$ and $\text{Zn}_2\text{Cl}_6^{2-}$ provides the former anion to the monomeric titanium cation and the latter dianion to $\text{V}_2\text{Cl}_3(\text{THF})_6^+$.

Structural Comparisons. Tetrahedral zinc anions of the sort ZnCl_3L^- have been seen in $\text{KZnCl}_3\cdot 2\text{H}_2\text{O}$ ¹⁵ (and its bromide analogue¹⁶), in $\text{Cl}_3\text{Zn}(\mu\text{-Cl})\text{Zn}(\text{H}_2\text{O})$ (triethanolamine),¹⁷ in $[\text{MoOCl}(\text{dppe})_2][\text{ZnCl}_3(\text{acetone})]$,¹⁸ and in $(\text{C}_5\text{H}_{11})_2\text{SCH}_2\text{-ZnI}_3^-$.¹⁹ Relevant dimensions of these compounds are quite comparable to those in $\text{ZnCl}_3(\text{THF})^-$. For example, in $\text{ZnCl}_3(\text{acetone})^-$, average values are Zn–Cl = 2.23 Å and Zn–O = 2.12 Å.

It is evident from the structure²⁰ of *mer*- $\text{TiCl}_3(\text{THF})_3$ that Ti–O distances suffer a considerable trans effect, being longer when trans to chlorine (2.18 Å) than when trans to ether oxygen (2.09 Å). In this context, the Ti–O distances in *trans*- $\text{TiCl}_2(\text{THF})_4^+$ (average 2.08 Å) are quite reasonable. The 2.36 Å Ti–Cl distance in this cation matches well the corresponding distance (2.35 Å) in *mer*- $\text{TiCl}_3(\text{THF})_3$. Another appropriate comparison compound is the *trans*- $\text{TiCl}_2(\text{H}_2\text{O})_4^+$ ion in $\text{Cs}_2\text{TiCl}_4\cdot 4\text{H}_2\text{O}$.²¹ The Ti–Cl distance (2.40 Å) and Ti–O distances (2.033 (5) and 2.046 (6) Å) are consistent with water being a somewhat better donor than THF. In contrast, much longer Ti–O distances are found in $[(\eta^8\text{-C}_8\text{H}_8)\text{TiCl}(\text{THF})_2]_2^{22}$ (2.25 Å) and $\text{CpTiCl}_2(\text{THF})_n$ (2.07 Å when $n = 1$ and 2.26 Å when $n = 2$).

The subtle variations of ether oxygen pyramidalities with

- (7) Bart, J. C. J.; Bassi, I. W.; Calcaterra, M.; Albizzati, E.; Giannini, U.; Parodi, S. Z. *Anorg. Allg. Chem.* **1981**, *482*, 121.
 (8) Bart, J. C. J.; Bassi, I. W.; Calcaterra, M.; Albizzati, E.; Giannini, U.; Parodi, S. Z. *Anorg. Allg. Chem.* **1983**, *496*, 205.
 (9) Natta, G.; Corradini, P.; Bassi, I. W. *J. Am. Chem. Soc.* **1958**, *80*, 755.
 (10) Thewalt, U.; Österle, F. *J. Organomet. Chem.* **1979**, *172*, 317.
 (11) Sobota, P.; Pluzinski, T.; Lis, T. *Polyhedron* **1984**, *3*, 45.

- (12) Sekutowski, D.; Jungst, R.; Stucky, G. D. *Inorg. Chem.* **1978**, *17*, 1848.
 (13) Sekutowski, D. G.; Stucky, G. D. *Inorg. Chem.* **1975**, *14*, 2192.
 (14) Sobota, P.; Utko, J.; Lis, T., submitted for publication.
 (15) Brehler, B.; Süssle, P. *Naturwissenschaften* **1963**, *50*, 517.
 (16) Föllner, H.; Brehler, B. *Acta Crystallogr. Sect. B* **1968**, *B24*, 1339.
 (17) Föllner, H. Z. *Anorg. Allg. Chem.* **1972**, *387*, 43.
 (18) Adam, V. C.; Gregory, U. A.; Kilbourn, B. T. *J. Chem. Soc., Chem. Commun.* **1970**, 1400.
 (19) Kilbourn, B. T.; Felix, D. *J. Chem. Soc. A* **1969**, 163.
 (20) Haldlovic, M.; Miklos, D.; Zikmund, M. *Acta Crystallogr. Sect. B* **1981**, *B37*, 811.
 (21) McCarthy, P. J.; Richardson, M. F. *Inorg. Chem.* **1983**, *22*, 2979.
 (22) van der Wal, H. R.; Overzet, F.; Van Oven, H. A.; DeBoer, J. L.; de Liefde Meijer, H. I.; Jellinek, F. *J. Organomet. Chem.* **1975**, *92*, 329.
 (23) Gambarotta, S.; Floriani, C.; Chiesi-Villa, A.; Guastini, C. *J. Am. Chem. Soc.* **1983**, *105*, 7295.

Ti-O distance (Table IV) can be interpreted as symptomatic of a (delocalized) tendency for four-electron donation (i.e., using both ether lone pairs), taking $\text{TiCl}_2(\text{THF})_4^+$ from the extreme of 13 toward 17 valence electrons. We shall expand on this idea in a subsequent description of a vanadium analogue of $[\text{TiCl}_2(\text{THF})_4][\text{ZnCl}_3(\text{THF})]$.

Acknowledgment. This work was supported by the National Science Foundation (Grant No. CHE 83-05281) and by the

Bloomington Academic Computing Service. We thank Stauffer Chemical Co. for material support and Scott Horn for skilled technical assistance.

Registry No. 1, 91797-55-6.

Supplementary Material Available: Listings of anisotropic thermal parameters, complete bond distances and angles, and observed and calculated structure factors (16 pages). Ordering information is given on any current masthead page.

Contribution from the Department of Chemistry, Georgetown University, Washington, D.C. 20057

Polyoxotungstate Anions Containing High-Valent Rhenium. 1. Keggin Anion Derivatives¹

FERNANDO ORTÉGA and MICHAEL T. POPE*

Received December 29, 1983

The heteropolytungstate anions $\alpha\text{-PW}_{11}\text{ReO}_{40}^{2-3-/4-}$, $\alpha\text{-SiW}_{11}\text{ReO}_{40}^{3-/4-/5-}$, $\text{BW}_{11}\text{ReO}_{40}^{4-/5-}$, and $\text{SiW}_{10}\text{Re}_2\text{O}_{40}^{2-/3-/4-}$ have been synthesized and isolated in the form of $(\text{C}_4\text{H}_9)_4\text{N}^+$ salts. The anions contain rhenium in oxidation states VII, VI, and V. X-ray powder diffraction establishes the monorhenate derivatives to have the Keggin heteropolyanion α -structure and the dirhenate, which was synthesized from $\beta\text{-A-SiW}_9\text{O}_{34}^{10-}$, probably to have the Keggin β -structure. Cyclic voltammograms of the monorhenates in CH_3CN show reversible redox processes coupling VII, VI, V, and IV oxidation states of rhenium. Electronic and, for Re(VI) anions, ESR spectra are reported. ESR parameters derived from simulated Q-band spectra are as follows: for $\text{PW}_{11}\text{ReO}_{40}^{3-}$, $g = 1.69, 1.73, 1.792$ and $a = 585, 324, 838$ G; for $\text{SiW}_{11}\text{ReO}_{40}^{4-}$, $g = 1.67, 1.69, 1.788$ and $a = 536, 291, 776$ G. The $(\text{CH}_3)_4\text{N}^+$ salt of $\text{SiW}_{11}\text{ReO}_{40}^{5-}$ shows electrochemically reversible oxidations to $\text{SiW}_{11}\text{ReO}_{40}^{4-}$ ($E_{1/2} = +0.28$ V vs. Ag/AgCl) and $\text{SiW}_{11}\text{ReO}_{40}^{3-}$ (+0.78 V) as well as pH-dependent reductions to $\text{SiW}_{11}\text{Re}^{\text{IV}}(\text{OH})\text{O}_{39}^{5-}$ and $\text{SiW}_{11}\text{Re}^{\text{III}}(\text{OH})_2\text{O}_{39}^{5-}$. Cyclic voltammograms of the dirhenate anions in CH_3CN show reversible redox processes coupling $\text{SiW}_{10}\text{Re}^{\text{VII}}\text{Re}^{\text{VI}}\text{O}_{40}^{2-}$, $\text{SiW}_{10}\text{Re}^{\text{VII}}\text{Re}^{\text{VI}}\text{O}_{40}^{3-}$, $\text{SiW}_{10}\text{Re}^{\text{VI}}\text{Re}^{\text{V}}\text{O}_{40}^{4-}$, $\text{SiW}_{10}\text{Re}^{\text{VI}}\text{Re}^{\text{V}}\text{O}_{40}^{5-}$, and either $\text{SiW}_{10}\text{Re}^{\text{V}}\text{O}_{40}^{6-}$ or $\text{SiW}^{\text{VI}}\text{W}^{\text{V}}\text{Re}^{\text{VI}}\text{Re}^{\text{V}}\text{O}_{40}^{6-}$. The electronic spectra of $\text{Re}^{\text{VII}}\text{Re}^{\text{VI}}$ - and $\text{Re}^{\text{VI}}\text{Re}^{\text{V}}$ -containing anions have bands assigned as intervalence charge transfer at 8300 and 8500 cm^{-1} , respectively. The X-band ESR spectrum of the $\text{Re}^{\text{VII}}\text{Re}^{\text{VI}}$ anion shows it to be a trapped-valence species at 77 K. The other dirhenate anions are ESR silent.

Heteropoly- and isopolyanions of the transition elements of groups 5 and 6 constitute a large class of complexes² that attract current interest because of their perceived analogies to metal oxide lattices and their potential and realized catalytic applications.³ Baker et al. recently discussed the characteristics of heteropolyanion-forming elements, notably their ionic radii (tetrahedral and octahedral coordination by oxide) and high positive charges.⁴ Post transition elements like Te^{6+} and I^{7+} have appropriate sizes and charges and may indeed form polyanion-like structures such as $\text{Co}_4\text{I}_3\text{O}_{24}\text{H}_{12}^{3-}$ but these atoms lack the ability to form the short terminal $\text{M}=\text{O}$ bonds that seem to be responsible for many of the redox and acid-base properties of "conventional" heteropolyanions.^{1a,b} Among the other transition elements, rhenium appears to be well suited for polyoxoanions: Re_2O_7 is a polymer with equal numbers of ReO_4 tetrahedra and ReO_6 octahedra; the oxide hydration product $\text{O}_3\text{ReOReO}_3(\text{H}_2\text{O})_2$ is a molecular species with corner-shared octahedral and tetrahedral rhenium atoms;⁵ short terminal $\text{Re}=\text{O}$ bonds are observed in complexes of Re(VII),

-(VI), and -(V) (e.g. ReOF_5 , ReOCl_4 , ReOCl_5^{2-}). Further, since ReO_3 and WO_3 are similar structurally, it would seem probable that one could prepare polytungstate anions in which one or more W(VI) atoms were replaced by Re(VI). Oxidation of these complexes could then lead to polyanions of uniquely low, perhaps zero, charge.

We report here the synthesis and properties of some rhenium-substituted polytungstates with the Keggin structure. Some years ago we described the ESR spectrum of $\alpha\text{-PW}_{11}\text{Re}^{\text{VI}}\text{O}_{40}^{4-}$,⁶ and Charreton and Meunier briefly reported the products of the reaction of ReCl_6^{2-} and $\alpha\text{-SiW}_{11}\text{O}_{39}^{8-}$ and $\alpha_2\text{-P}_2\text{W}_{17}\text{O}_{61}^{10-}$.⁷ The only other work with rhenium and polyanions appears to be solution studies of Re(V) with molybdate and molybdosilicate, from which the formation of several molybdorhenates was inferred.⁸

Experimental Section

Syntheses. The following salts were prepared according to published methods and were identified by infrared spectroscopy and, in the case of the heteropolyanions, by polarography: $\alpha\text{-}[(n\text{-C}_4\text{H}_9)_4\text{N}]_4\text{H}_3\text{PW}_{11}\text{O}_{39}$,⁹ $[(n\text{-C}_4\text{H}_9)_4\text{N}]\text{ReOBr}_4$,¹⁰ $\alpha\text{-K}_8\text{SiW}_{11}\text{O}_{39}\cdot 12\text{H}_2\text{O}$,¹¹ $[\text{ReO}_2(\text{py})_4]\text{Br}\cdot 2\text{H}_2\text{O}$,¹² $\text{K}_9\text{BW}_{11}\text{O}_{39}\cdot x\text{H}_2\text{O}$,¹³ $\beta\text{-Na}_9\text{HSiW}_9\text{O}_{34}\cdot 23\text{H}_2\text{O}$.¹⁴

(1) Ortéga, F. Ph.D. Thesis, Georgetown University, 1982.

(2) (a) Pope, M. T. "Heteropoly and Isopoly Oxometalates"; Springer-Verlag: New York, 1983. (b) Porai-Koshits, M. A.; Atovmyan, L. O. *Russ. J. Inorg. Chem. (Engl. Transl.)* **1981**, *26*, 1697. (c) Spitsyn, V. I.; Kazanskii, L. P.; Torchenkova, E. A. *Sov. Sci. Rev. Sect. B* **1981**, *3*, 111. (d) Tsigdinos, G. A. *Top. Curr. Chem.* **1978**, *76*, 1. (e) Weakley, T. J. R. *Struct. Bonding (Berlin)* **1974**, *18*, 131. (f) Evans, H. T., Jr. *Perspect. Struct. Chem.* **1971**, *4*, 1.

(3) Baker, L. C. W. "Advances in the Chemistry of Coordination Compounds"; Kirschner, S., Ed.; MacMillan: New York, 1961; p 604. Misono, M. *Chem. Uses Molybdenum, Proc. Conf., 4th* **1982**, 289. Ai, M. *J. Catal.* **1981**, *7*, 88. Kozhevnikov, I. V.; Matveev, K. I. *Russ. Chem. Rev. (Engl. Transl.)* **1982**, *51*, 1075; *Appl. Catal.* **1983**, *5*, 135.

(4) Baker, L. C. W.; Lebiada, L.; Grochowski, J.; Mukherjee, H. G. *J. Am. Chem. Soc.* **1980**, *102*, 3274.

(5) Beyer, H.; Glemser, O.; Krebs, B. *Angew. Chem., Int. Ed. Engl.* **1968**, *7*, 295.

(6) Meiklejohn, P. T.; Pope, M. T.; Prados, R. A. *J. Am. Chem. Soc.* **1974**, *96*, 6779.

(7) Charreton, B.; Meunier, R. C. R. *Hebd. Seances Acad. Sci., Ser. C* **1974**, *275*, 945.

(8) Semenovskaya, E. N. In "Issledovanie Svoistu i Primenenie Geteropolikislot v Katalize" (Investigations of the Properties and Applications of Heteropoly Acids in Catalysis); Akademiya Nauk SSSR, Institut Kataliza: Novosibirsk, 1978; p 96. Semenovskaya, E. N.; Basova, E. M. *J. Anal. Chem. USSR (Engl. Transl.)* **1982**, *37*, 1565.

(9) Ho, R. K. C. Ph.D. Thesis, Columbia University, 1979.

(10) Cotton, F. A.; Lippard, S. J. *Inorg. Chem.* **1966**, *5*, 1.

(11) Těžď, A.; Hervě, G. *J. Inorg. Nucl. Chem.* **1977**, *39*, 999.

(12) Johnson, N. P.; Taha, F.; Wilkinson, G. *J. Chem. Soc.* **1964**, 2614.

(13) Souchay, P. *Ann. Chim. Anal.* **1945**, *20*, 96.